Solvent Control in the Protonation of [Cp*Mo(dppe)H3] by CF3COOH

Pavel Dub, Miguel Baya, Jennifer Houghton, Natalia v. Belkova, Jean-Claude Daran, Rinaldo Poli, Lina M. Epstein, Elena S. Shubina

Solvent control in the protonation of [Cp*Mo(dppe)H_3] by CF_3COOH.

Pavel A. Dub,[a,b] Miguel Baya,[a] Jennifer Houghton,[a] Natalia V. Belkova,[b] Jean-Claude Daran,[a] Rinaldo Poli,*[a] Lina M. Epstein,[b] Elena S. Shubina*[b]

[a]*Laboratoire de Chimie de Coordination, UPR CNRS 8241 liée par convention à l'Université Paul Sabatier et à l'Institut National Polytechnique de Toulouse, 205 Route de Narbonne, 31077 Toulouse Cedex, France*

[b]*Nesmeyanov Institute of Organoelement Compounds, Russian Academy of Sciences, Vavilov Street 28, 119991 Moscow, Russia*

Proofs to:

Rinaldo Poli

Tel: +33-561333173

Fax: +33-561553003

E-mail: poli@lcc-toulouse.fr

Summary

The outcome of the reaction between $Cp^*Mo(dppe)H_3$ [dppe = 1,2-bis(diphenylphosphino)ethane] and trifluoroacetic acid (TFA) is highly dependent on the solvent and the TFA/Mo ratio. The new dihydride compound $Cp^*Mo(dppe)H_2(O_2CCF_3)$ is obtained selectively when the reaction is carried out in aromatic hydrocarbons (benzene, toluene) using ≤1 equiv of TFA, and is also the end product in THF or MeCN independent of the TFA/Mo ratio. In benzene/toluene, use of an excess amount of the acid has a profound effect, resulting in the formation of the tetrahydrido complex $[Cp^*Mo(dppe)H_4]^+$, which does not further evolve to the dihydrido product. Monitoring the reaction by NMR and IR under different conditions (solvent, temperature, TFA/Mo ratio) reveals the rapid establishment of an equilibrium between the dihydrogen bonded adduct, $Cp^*Mo(dppe)H_3\cdots HOOCCF_3$, the ion paired proton transfer product, $Cp^*Mo(dppe)H_4^+\cdots{}^-OOCCF_3$, and the separated ions, followed by a slower irreversible transformation to the final dihydride product with H_2 evolution. The activation parameters of the H_2 evolution and M-OR product formation have been determined. Excess TFA in low polarity solvents stabilizes the separated charged species by forming the homoconjugate anion $[CF_3COO(HOOCCF_3)_n]^-$. The effect of the solvent on the course of the reaction is interpreted in terms of the differing polarity, H-bonding ability, and coordinating power of the different solvent molecules.

Keywords: Molybdenum, hydride ligands, proton transfer, dihydrogen bonding, trifluoroacetate ligand

Introduction

It is now well established that a common proton transfer pathway from a proton donor HA to a transition metal hydride complex involves the initial attack of HA on the hydride ligand with formation of a dihydrogen bonded adduct, MH···HA, followed by proton transfer and production of a non-classical dihydride (dihydrogen complex) product, $M(\eta^2\text{-}H_2)^+$. The establishment of a hydrogen bonded ion pair between the non-classical cation and its counteranion decreases the stability of the $M(\eta^2\text{-}H_2)^+$ complex and favors its transformation into a classical polyhydride or organyloxo (if X = OR) species (Scheme 1).[1]

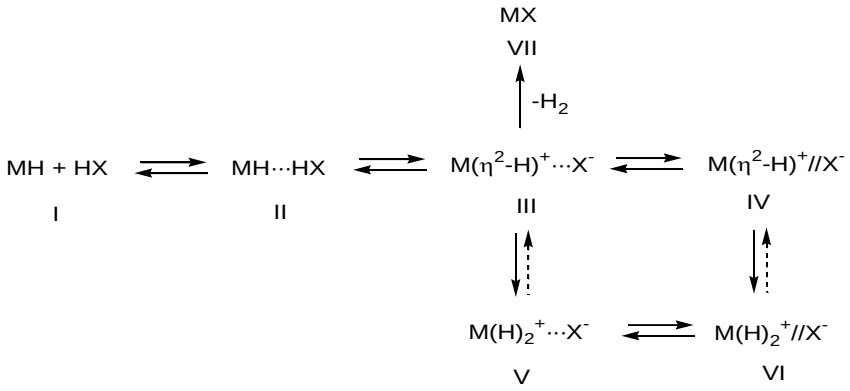

Scheme 1

The formation of $M(\eta^2\text{-}H_2)^+\cdots X^-$ ion pairs (**III**, $X^- = CF_3COO^-$, ArO^-, R^FO^-), stabilized by hydrogen bonds between the dihydrogen ligand and counteranions, was detected for $CpRuH(CO)(PCy_3)$,[2, 3] PP_3MH_2 [$PP_3 = P(CH_2CH_2PPh_2)_3$][4] and Cp*MH(dppe) (M = Fe,[5] Ru[6]) complexes by IR and UV-visible spectroscopy. The ion pair stability increases with the proton accepting ability of the anion.[3]

Proton transfer may also be assisted by a second molecule of the proton donor HX, depending on the acid strength. In this case, the conjugate base X^- in species **III-VI** may be present in the form of the homoconjugate anion, XHX^-. We have recently shown that the

irreversible isomerization of Cp*M(η^2-H_2)(dppe)$^+$ complexes (M = Fe,[5] Ru[6]) into classical *trans*-dihydride species occurs upon dissociation of the M(η^2-H_2)$^+\cdots$XHX$^-$ ion pair (*i.e.* **III** to **IV**). This is indicated by difference in temperature at which the M(η^2-H_2)$^+$ → M(H)$_2^+$ isomerization process can occur depending on the counteranion: higher temperatures are necessary to induce isomerization in the presence of more basic anions (greater ion pair stability). Additionally, the isomerization rate constant does not depend on the anion nature.[7, 8] In some cases, the non-classical to classical rearrangement (**III** to **V**, or **IV** to **VI**) is a reversible process.[9]

In many cases, however, basic anions (X$^-$ = RO$^-$, RCOO$^-$) tend to displace H_2 from the transition metal coordination sphere, yielding organyloxo products (*i.e.* **VII**). This is the case for the protonation of (triphos)ReH(CO)$_2$,[10] Re(CO)H_2(NO)(PR$_3$)$_2$,[11] and the above mentioned CpRuH(CO)(PCy$_3$),[2] for which corresponding M(η^2-H_2)$^+$X$^-$ complexes could be isolated as BF_4^- salts which evolved into MX species in the presence of fluorinated alcohols or carboxylic acids. This reaction proceeds intra-molecularly without the hydrogen bonded ion pair dissociation.[2] Most of the M-OR complexes were only characterized in solution, two examples of isolated compounds being ReH(OC$_6$H$_4$NO$_2$)(CO)(NO)(PMe$_3$)$_2$[11] and (triphos)Re(CO)$_2$-(OCOCH$_2$Cl).[10] In addition to the counteranion nature, temperature and solvent polarity could be used to control the stability of the M(η^2-H_2)$^+$ species and the proton transfer equilibrium position. For example, the substantial increase of the dielectric constant of the Freon mixture ($CDCl_2F/CDF_3$ 2:1) at low temperatures was reported to assist the proton transfer to Cp*RuH$_3$(PCy$_3$) yielding [Cp*Ru(H)$_2$(η^2-H_2)(PCy$_3$)]$^+$OR$^-$.[12] However, the influence of the medium on the H_2 release process was not studied in detail.

In contrast to all the above described systems, the protonation of the trihydridomolybdenum complex Cp*Mo(dppe)H_3 gives, via the intermediate formation of a dihydrogen bonded complex, the cationic classical tetrahydride complex [Cp*Mo(dppe)H_4]$^+$ (**V**/**VI**), without the detection of a nonclassical isomer, [Cp*Mo(dppe)(η^2-H_2)H_2]$^+$ (**III**/**IV**).

Theoretical calculations, however, located the latter complex on the proton transfer potential energy surface, with a very low energy barrier for the intramolecular rearrangement.[13] Facile access to a nonclassical isomer is evidenced by the evolution of H_2 from $[Cp^*Mo(dppe)H_4]^+$ at ambient temperature. We now report new results on the protonation of $Cp^*Mo(dppe)H_3$ using trifluoroacetic acid (TFA) in various solvents of different coordinating (in particular H-bonding) ability and polarity: benzene, toluene, THF, CH_2Cl_2 and MeCN. These reactions lead to the formation of a new hydride product with a coordinated trifluoroacetate anion. We will show how subtle changes of the protonation medium may drastically effect the reactivity of $Cp^*Mo(dppe)H_3$ and the stability of its protonation product.

Results

Since the results of previous investigations into the protonation of $Cp^*Mo(dppe)H_3$[13-15] serve as basis for the new findings described in this paper, we summarize here the salient points that emerge from those studies. (*i*) The trihydride complex has a high basicity factor (E_j = 1.42±0.02), placing it in the category of the most hydridic complexes known. (*ii*) As mentioned in the introduction, the interaction with HBF_4 in non coordinating or weakly coordinating solvents (ether, THF) leads directly to the tetrahydride complex $[Cp^*Mo(dppe)H_4]^+$, without the detection of a nonclassical intermediate, although its presence is suggested by the theoretical calculations. (*iii*) $[Cp^*Mo(dppe)H_4]^+BF_4^-$ is unstable and rapidly loses dihydrogen; in MeCN, this process leads to the formation of the solvent stabilized complex $[Cp^*Mo(dppe)H_2(MeCN)]^+$. (*iv*) The interaction with weaker proton donors (the fluorinated alcohols CH_2FCH_2OH, CF_3CH_2OH, and $(CF_3)_2CHOH$) in low polarity solvents (e.g. THF, CH_2Cl_2) at low temperatures leads to the observation of intermediate hydrogen bonded adducts. Infrared spectral analysis, in combination with theoretical calculations, indicates that one of the hydride ligands of $Cp^*Mo(dppe)H_3$ takes part in hydrogen bonding. (*v*) Proton transfer from the dihydrogen-

bonded adduct yields, without the observable intervention of a second HA molecule in the rate determining step, the tetrahydride product as a 1:1 ion pair stabilized by a hydrogen bond between the cation and the anion, $[Cp^*Mo(dppe)H_4]^+\cdots A^-$, as established for HA = *p*-nitrophenol and CF_3CH_2OH. The proton transfer reaction is equilibrated for these weaker proton donors. (*vi*) On a longer time scale, the tetrahydride product $[Cp^*Mo(dppe)H_4]^+$ obtained using HA = CF_3CH_2OH evolves at ambient temperature by release of two H_2 molecules to form the hydride-free product $Cp^*Mo(dppe)(OCH_2CF_3)$, probably stabilized by coordination of a second alcohol molecule, $Cp^*Mo(dppe)(OCH_2CF_3)(CF_3CH_2OH)$. The above observations are summarized in Scheme 2.

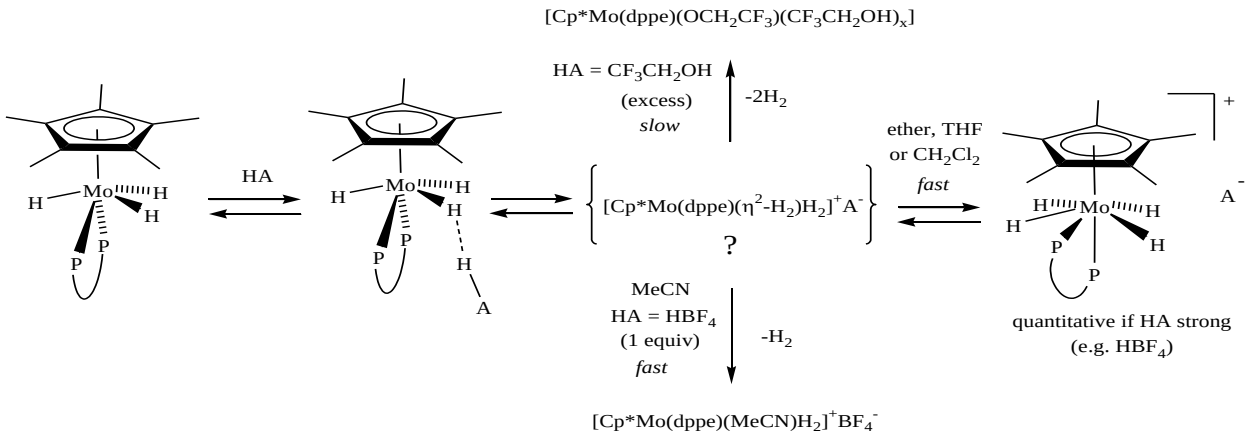

Scheme 2

(a) Protonation in benzene/toluene: formation of compound $Cp^*Mo(dppe)H_2(O_2CCF_3)$.

The room temperature reaction between $Cp^*MoH_3(dppe)$ and *strictly* 1 equivalent of TFA in toluene led selectively to a new dihydride complex, $Cp^*Mo(dppe)H_2(O_2CCF_3)$, as seen in Equation 1. The parallel formation of free H_2 was confirmed by ^1H NMR monitoring (characteristic resonance at δ 4.58). The new hydride compound was isolated and fully characterized. It is quite stable in aromatic solvents, decomposing very slowly with generation of free dppe (identified by its ^{31}P resonance at δ -12.9) and other unidentified products that do

not contain hydride ligands. Ca. 13 % of the product decomposed after 22 hours at room temperature.

$$Cp^*Mo(dppe)_3H_3 + TFA \longrightarrow Cp^*Mo(dppe)H_2(O_2CCF_3) + H_2$$

Equation 1

The compound is characterized by a hydride resonance centered at δ -5.08, with a relative intensity corresponding to two protons, only slightly displaced with respect to the hydride resonance of $Cp^*Mo(dppe)H_3$ at δ -5.16. The $^{31}P\{^1H\}$ spectrum shows a resonance at δ 76.9, which becomes a triplet when selectively decoupled from the dppe proton resonance, confirming the presence of two hydride ligands. The shape of the hydride resonance suggests the occurrence of a dynamic process. A variable temperature NMR investigation gave further information about this process and also provided longitudinal relaxation times for the hydride resonances. The shape of the ^1H NMR resonances in the hydride region as a function of temperature is shown in Figure 1(a). Cooling resulted in broadening and eventual decoalescence (225 K), yielding two broad resonances in a 1:1 ratio at δ -4.19 and -6.24. The more upfield resonance starts to resolve into a doublet at the lowest temperature, indicating coupling (J ca. 72 Hz) to another I = ½ nucleus, probably one of the two P donors that therefore appear to be inequivalent. This inequivalence was demonstrated by the variable temperature $^{31}P\{^1H\}$ NMR investigation, see Figure 1(b), decoalescence being observed at T < 233 K to yield two resonances in an approximate ratio of 1:1. No P-P coupling can be discerned from the spectra. The ^{31}P data were used in a lineshape analysis, from which the activation parameters of $\Delta H^{\ddagger} = 6.4 \pm 0.4$ kcal mol^{-1} and $\Delta S^{\ddagger} = 10 \pm 2$ cal K^{-1} mol^{-1} were calculated using an Eyring analysis (see Supporting Information). The line shape analysis of the ^1H resonance was complicated by the lack of knowledge of J_{HP} data due to broadness in the low temperature spectra, but a simulation using the rate constant obtained from the ^{31}P spectrum and a reasonable guess for the J_{HP} values gave a

reasonable fit above coalescence, suggesting that the same mechanism is responsible for both H and P exchange processes. A possibility for this mechanism is illustrated in Scheme 3. The T_1 value for the hydride resonance remains rather high throughout the temperature range (see Supporting Information), characteristic of a classical dihydride, with a minimum of 510 ms before decoalescence. For comparison, the T_{1min} of complex $[Cp^*Mo(dppe)H_4]^+$ is 174 ms for the BF_4^- salt and 191 ms when obtained by proton transfer from TFE (these measurements were carried out at 400 MHz).[13]

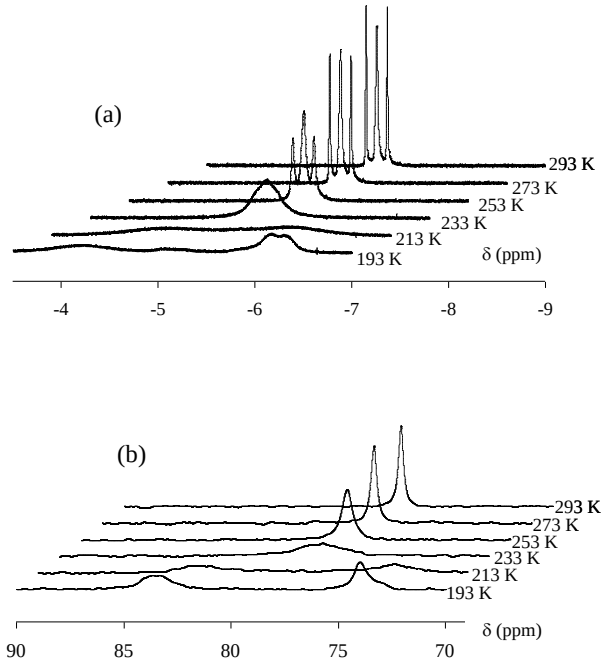

Figure 1. Variable temperature spectra for compound $Cp^*Mo(dppe)H_2(O_2CCF_3)$ in $C_6D_5CD_3$. (a) ^1H NMR (500 MHz). (b) $^{31}P\{^1H\}$ NMR (202 MHz).

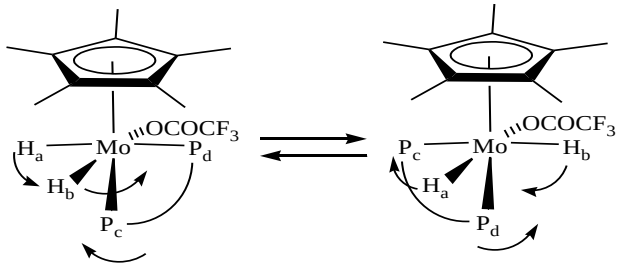

Scheme 3

The chemical composition of the product was confirmed by a single crystal X-ray analysis. The coordination geometry, shown in Figure 2, corresponds to a rather severely distorted octahedron if the Cp* ligand is considered to occupy a single coordination position at the ring centroid. This distortion is caused by steric repulsion between the Cp* and dppe ligands and by the small size of the two hydride ligands, which force the pseudo-axial (trans to the Cp*) phosphorus donor to move up into the wedge of the two Mo-H bonds. The CNT-Mo-P1 angle (122.648(13)°) is substantially greater than the CNT-Mo-O1, CNT-Mo-H1 and CNT-Mo-H2 angles (119.74(4)°, 98.5(10)° and 96.9(9)°, respectively), whereas the CNT-Mo-P2 angle (144.369(14)°) is much smaller than 180°. A similar distortion was observed in the structure of the related $[Cp^*Mo(dppe)H(MeCN)_2]^{2+}$ complex.[14] The other notable feature is the monodentate coordination of the trifluoroacetate ligand, which occupies a pseudo-equatorial position *cis* to the P1 and H1 donors and *trans* to H2. The Mo-O1 bond length (2.2008(15) Å) is unexpectedly longer than those found in other Mo monodentate carboxylate derivatives in the same or lower oxidation state, *e.g.* 2.167(4) Å found in $Cp^*Mo^{II}(CO)(PMe_3)_2(O_2CMe)$,[16] 2.102(3) and 2.092(3) Å found in $CpMo^{III}(\eta^4\text{-}C_4H_6)(O_2CCF_3)_2$,[17] and 2.113 (4) and 2.102 (4) Å found in $Cp_2Mo^{IV}(O_2CPh)_2$.[18] Another interesting feature is the similar C8-O1 (1.249(3) Å) and C8-O2 (1.221(3) Å) distances (bond difference Δ = 0.028 Å). These are not quite as long or short, respectively, as expected for localized single and double bonds. For instance, the recently determined structure of Ph_3CCH_2COOH shows clearly defined C-O [1.304(3) Å] and C=O [1.203(3) Å] bonds (Δ = 0.101 Å) with no obvious sign of hydrogen atom disorder.[19] The monodentate carboxylate C-O distances in the above mentioned examples show larger differences between C=O and C-O bond lengths, although not quite as large as those found in free carboxylic acids, namely 1.277(8) *vs.* 1.212(8) Å (Δ = 0.065 Å) for $Cp^*Mo^{II}(CO)(PMe_3)_2$-(O_2CMe),[16] 1.276(5) and 1.255(5) *vs.* 1.200(5) and 1.192(6) Å (Δ = 0.076 and 0.063 Å) for $CpMo^{III}(\eta^4\text{-}C_4H_6)(O_2CCF_3)_2$,[17] and 1.281(8) and 1.300(8) vs. 1.208(8) and 1.210(8) Å (Δ =

0.073 and 0.090 Å) for $Cp_2Mo^{IV}(O_2CPh)_2$.[18] The above combined evidence indicates a significant ionic contribution to the bond between the Mo center and the monodentate anion, which then continues to promote some electronic delocalization between the two C-O bonds. Other relevant structural parameters are listed in Table 1.

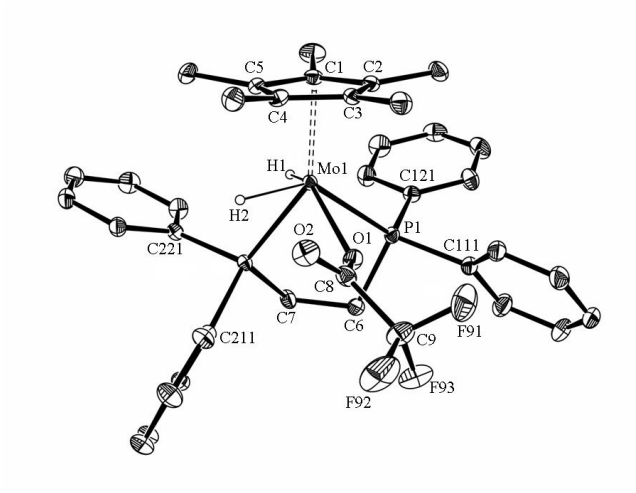

Figure 2. ORTEP view of compound $Cp^*Mo(dppe)H_2(OCOCF_3)$. For the sake of clarity, the H atoms are not shown, except for the two hydride ligands. The thermal ellipsoids are drawn at the 30% probability level.

Compound $Cp^*Mo(dppe)H_2(OCOCF_3)$ exhibits two intense overlapping ν^{as}_{OCO} bands in the IR spectrum, the frequencies and relative intensities of which are solvent dependent (see Table 2). As the solvent polarity increases, A_{low}/A_{high} decreases and $\Delta\nu = (\nu_{high} - \nu_{low})$ increases. The same behavior was observed previously for $CpM(CO)_2(OCOR)$ complexes (M = Fe, Ru)[20] and was explained by the presence of a Fermi resonance between the fundamental ν^{as}_{OCO} stretching vibration and an overtone or combination band of very close frequency. The larger intensity ratio observed in CH_2Cl_2 could be explained by the different nature of the solute-solvent interaction, since this solvent could act as a proton donor and form hydrogen bonds with carboxyl group coordinated to the metal.

(b) Protonation in benzene/toluene: evolution with time.

The ^{1}H NMR monitoring of the Cp*Mo(dppe)H_3-TFA reaction in C_6D_6 at different TFA/Mo ratios at room temperature was most enlightening. Figure 3a shows the spectrum of the starting material before TFA addition.[21]

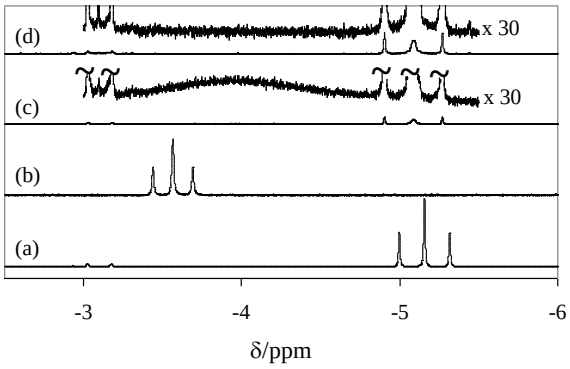

Figure 3. ^{1}H NMR (300 MHz) monitoring of the reaction between Cp*Mo(dppe)H_3 and TFA in C_6D_6 (290 K). (a) Starting material before the TFA addition; (b) immediately after the TFA addition (10 equiv) (c) immediately after the TFA addition (1 equiv); (d) after 3.5 h from spectrum (c).

When using a 10-fold excess of TFA, the tetrahydrido complex [Cp*Mo(dppe)H_4]$^+$ was the only observed product, Figure 3b. This is characterized by a hydride triplet resonance at -3.57 ppm (J_{HP} = 37.9 Hz) in the ^{1}H NMR spectrum and by a ^{31}P resonance at 72.3 ppm in C_6D_6, quite close to the values previously reported for the BF_4^- salt in $CDFCl_2$ at -60°C.[14] In agreement with the literature, decomposition takes place at room temperature (90% after ca. 25 min), without yielding any hydride containing product. This decomposition was not investigated in any further detail.

For the 1:1 reaction, a broad resonance was initially present in the hydride region at an intermediate position between those of the trihydride and tetrahydride complexes, in addition to the final product resonance (Figure 3c). The position and shape of the broad resonance depends on the TFA/Mo ratio and on the temperature (*vide infra*). The ^{31}P{^{1}H} spectrum at room temperature exhibits two small and broadened resonances at the characteristic positions of the trihydride complex (δ 91.4) and the tetrahydride protonation product (δ 72.3),[22] in addition to

the sharp resonance of the Cp*Mo(dppe)$H_2(O_2CCF_3)$ product at δ 76.9 and a minor contaminant resonance.[21] This suggests that the broad ^{1}H NMR resonance results from a rapid degenerate exchange between the starting complex Cp*Mo(dppe)H_3, which is not completely consumed, and its protonation product, Cp*Mo(dppe)H_4^+. This exchange will be addressed in further detail in the next section. Given the larger chemical shift difference between the ^{31}P resonances, the shape of ^{31}P NMR spectrum is much closer to the slow exchange limit than that of the ^{1}H NMR spectrum. After a few hours at room temperature (or upon brief warming to ca. 40°C), the broad band disappears and the resonance corresponding to Cp*Mo(dppe)$H_2(OCOCF_3)$ increases in intensity (Figure 3d). These observations reveal the presence of an equilibrium between the tetrahydride complex and the starting trihydride complex, followed by a slow irreversible conversion to the final product by H_2 loss.

A variable temperature study of the reaction mixture in $C_6D_5CD_3$, carried out immediately after mixing the reagents in a 1:1 ratio, confirmed the above assignments. The hydride resonance of the dihydride product evolved as discussed above (Figure 1a), whereas the broad resonance at –3.63 ppm decoalesced at T < 270 K to yield two resonances at the expected positions of Cp*Mo(dppe)H_3 and Cp*Mo(dppe)H_4^+. The incomplete protonation in the presence of a stoichiometric amount of TFA shows that the protonation process is at equilibrium using this particular proton donor. Both complexes exhibit sharp resonances when alone and also when mixed together with Cp*Mo(dppe)$H_2(OCOCF_3)$. Interestingly, the hydride resonance of Cp*Mo(dppe)H_4^+ broadens again at temperatures < 240 K, but does not decoalesce. On the other hand, the BF_4^- salt of this complex was previously reported to retain sharp lines in the ^{1}H and ^{31}P NMR spectra down to -90°C, indicating rapid equilibration between the inequivalent H sites.[14] This suggests that the hydride scrambling process is slowed down by hydrogen bonding between Cp*Mo(dppe)H_4^+ and CF_3COO^-.

The reaction with 3 equiv of TFA resulted in the observation of a sharp resonance at the chemical shift of the tetrahydride complex (indicating essentially complete disappearance of the

starting trihydride reagent) and no significant amount of the dihydride product. The subsequent addition of two equivalents of Et_2NH to this solution led to the formation of complex $Cp^*Mo(dppe)H_2(OCOCF_3)$ cleanly and quantitatively. When using 1.5 equivalents of TFA, rather sharp resonances for the tetrahydrido complex and the final dihydrido product were initially observed by ^1H NMR monitoring, but the latter was once again the only observable species remaining at end of the reaction (ca. 30 min at 290 K). When using only 0.5 equiv of TFA, on the other hand, a broad resonance was again initially present, but its chemical shift was closer to that of the starting hydride complex, see Figure 4. This is as expected, because the equilibrium mixture of the rapidly exchanging $Cp^*Mo(dppe)H_3$ and $[Cp^*Mo(dppe)H_4]^+$ complexes is now richer in the former. The formation of the final dihydride product was slower (equilibrium was attained in ca. 2 h at 290 K), and ca. 50% of the initial trihydride remained unreacted. As the $[Cp^*Mo(dppe)H_4]^+$ reacted to yield $Cp^*Mo(dppe)H_2(OCOCF_3)$, the resonance corresponding to $Cp^*Mo(dppe)H_3$ sharpened. The addition of excess TFA to a solution containing $Cp^*Mo(dppe)H_2(OCOCF_3)$ does not lead to any reaction, in particular no tetrahydride resonance was observed under these conditions.

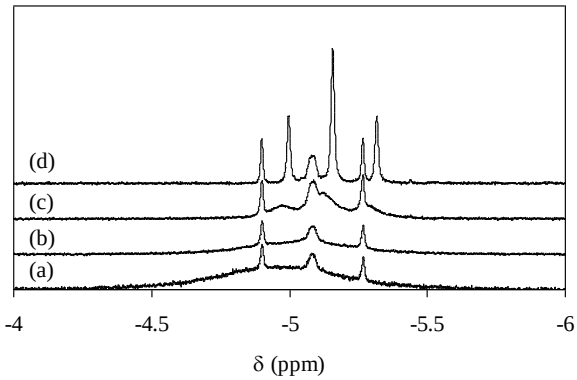

Figure 4. ^1H NMR (300 MHz) monitoring of the reaction between $Cp^*Mo(dppe)H_3$ and TFA (1:0.5 ratio) in C_6D_6 (290 K). (a) Recorded immediately; (b) after 7 min; (c) 28 min; (d) 155 min.

We have also investigated the reaction between Cp*Mo(dppe)H_3 and CF_3COOD (1 equivalent) by ^1H NMR in $C_6D_5CD_3$. The reaction progresses in an essentially identical manner to that when CF_3COOH is used: immediate observation of the virtual triplet at δ -5.25 due to the final product and a broad resonance centred at ca. δ -3.6. The latter disappears upon brief warming to ca. 40°C. However, the NMR shows the formation of H_2 and HD in ca. 3:1 ratio. This is not surprising, since all hydride positions in the tetrahydride complex are readily scrambled, therefore the elimination of H_2 from the $[Cp^*Mo(dppe)H_3D]^+$ cation will be statistically favored. The molybdenum product resulting from this reaction should therefore contain both H and D. The hydride resonance does not show evidence for the presence of isotopomers, probably because the isotope shift is too small. The formation of deuterated product(s), Cp*Mo(dppe)HD(O_2CCF_3) and/or Cp*Mo(dppe)D_2(O_2CCF_3), however, was confirmed by a ^2H NMR study, which revealed a binomial triplet resonance at δ -5.9 with J_{PD} = 7.7 Hz.

(c) Protonation in other solvents: NMR study.

The solvent has a significant effect on the course of the protonation reaction. The behavior in THF-d_8 is similar but not identical to that in aromatic hydrocarbons (see Figure 5): use of a (sub)stoichiometric amount of the acid initially yields a broad hydride resonance (Figure 5b). Time evolution at these ratios leads to sharpening of the signals as the irreversible H_2 elimination and Cp*Mo(dppe)H_2(O_2CCF_3) formation takes place, a similar process to that shown in Figure 4 for the benzene solution. When the sample corresponding to Figure 5b was treated with additional TFA (total: 1.5 equiv) quantitative formation of the dihydride product occurred (Figure 5c). Use of a large excess (10 equiv) of CF_3COOH affords a sharp triplet corresponding to the tetrahydrido cation and a strong resonance for the Cp*Mo(dppe)H_2(O_2CCF_3) product (Figure 5d). As in C_6D_6 or $C_6D_5CD_3$, a broad resonance is not obtained at this ratio. However,

with time, the tetrahydride resonance disappears and the dihydride resonance increases in THF-d_8 (Figure 5e), whereas in the analogous benzene solution decomposition occurs without formation of the dihydride product, as stated above.

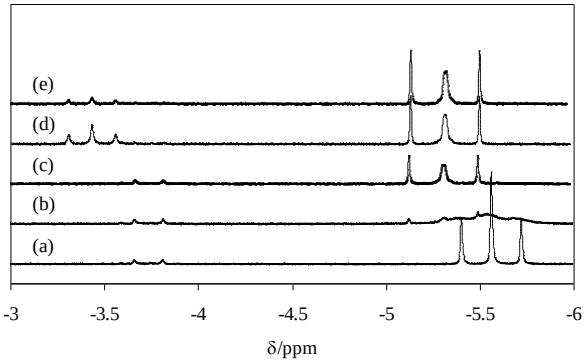

Figure 5. ^{1}H NMR (300 MHz) monitoring of the reaction between Cp*Mo(dppe)H_3 and TFA in THF-d_8 at 290K: (a) before the TFA addition; (b) TFA/Mo = 0.5, 8 min; (c) further addition of 1 equiv to sample (b): TFA/Mo = 1.5, 30 min; (d) TFA/Mo = 10, immediately after the addition; (e) after 13 min from sample (d). The doublet resonance at δ -3.73 belongs to the Cp*Mo(κ^1-dppe)H_5 contaminant.[14]

THF was found to be a suitable solvent in which to probe the nature of the degenerate exchange between CpMo(dppe)H_3 and [Cp*Mo(dppe)H_4]$^+$, by repeating the protonation in the presence of HBF_4 instead of CF_3COOH (the BF_4^- salt of the tetrahydride product is soluble in THF, but precipitates from toluene or benzene). If the exchange takes place bimolecularly via a symmetrical [Cp*(dppe)H_3Mo···H···MoH_3(dppe)Cp*]$^+$ transition state, the lineshape of the signal will not depend on the nature of the acid. On the other hand, a unimolecular pathway involving the conjugate base of the proton donor should yield a slower exchange rate for the BF_4^- sample, because this is a much weaker base than CF_3COO^-. The NMR study of a 2:1 Cp*Mo(dppe)H_3/HBF_4 mixture provides evidence in favor of the unimolecular pathway. As can be seen in Figure 6, addition of 0.5 equiv of HBF_4 results in a decrease in the Cp*Mo(dppe)H_3 resonance and the appearance of the [Cp*Mo(dppe)H_4]$^+$ resonance, plus a weak triplet resonance at δ -5.65 (J_{HP} = 53.5 Hz), whilst the doublet resonance of the Cp*Mo(κ^1-dppe)H_5 contaminant

remains unchanged. The trihydride and tetrahydride complexes give separated sharp resonances, contrary to the same situation in the presence of trifluoroacetate anion in the same solvent (Figure 5b). This clearly demonstrates that the anion determines the rate of degenerate exchange. This exchange process therefore involves the hydrogen bonded ion pair $[Cp^*Mo(dppe)H_4]^+\cdots^-OCOCF_3$ and the dihydrogen bonded trihydride $Cp^*Mo(dppe)H_3\cdots HOCOCF_3$, the latter being in further rapid equilibration with free trihydride and TFA. Analogous broadening phenomena for hydride signals as a consequence of dihydrogen bonding and equilibrated proton transfer were noted previously in other cases, although the broadening effect was limited to a few Hz in most cases.[2, 23]

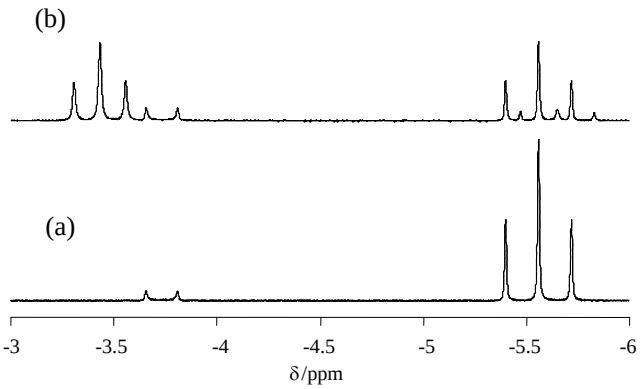

Figure 6. ^1H NMR study of a $Cp^*Mo(dppe)H_3/HBF_4$ mixture in THF-d_8: (a) starting compound; (b) 21 min after the addition of 0.5 equiv of HBF_4. The doublet resonance at δ -3.73 belongs to the $Cp^*Mo(\kappa^1\text{-dppe})H_5$ contaminant.[14]

The new triplet resonance at δ -5.65 in Figure 6 is assigned to complex $[Cp^*Mo(dppe)H_2(THF)]^+$. It is associated with a new $^{31}P\{^1H\}$ resonance at δ 70.7. For comparison, the related $[Cp^*Mo(dppe)H_2(MeCN)]^+$ complex, obtained from the protonation of $Cp^*Mo(dppe)H_3$ by HBF_4 in MeCN,[14] displays a proton resonance at δ -5.50 (J_{P1} = 51 Hz, J_{P2} = 52 Hz) and a phosphorus resonance at δ 78.1. NMR monitoring shows that this resonance grows while the resonance of the tetrahydride product simultaneously decreases. Interesting features to note are: (*i*) this cationic THF adduct is not observed in the protonation experiment with

CF_3COOH; (*ii*) the rate of disappearance of the tetrahydride complex is much slower in the presence of the BF_4^- anion than in the presence of the CF_3COO^- anion (*cf.* Figure 6 with Figure 5); (*iii*) conversion to the THF solvent adduct appears to be much slower than the analogous reaction in MeCN, which was reported to lead to vigorous gas evolution and quantitative production of the MeCN complex within 60 min.[14]

When using CH_2Cl_2 as solvent, the initially formed tetrahydride complex displayed a sharper resonance, even when as little as 0.5 equiv of the acid was used. The formation of minor amounts of $Cp^*Mo(dppe)H_2(O_2CCF_3)$ was also detected (ca. 10% for the 1 equiv experiment). In this solvent, however, the interpretation of the data is difficult because of the instability of the starting material, the cationic tetrahydride intermediate, and the product (24% decomposition within 1 hour at RT).

Finally, the results of the protonation with TFA (0.5 and 1 equiv) in MeCN-d_3 at room temperature are shown in Figure 7. In both cases, the immediate formation of $Cp^*Mo(dppe)H_2(O_2CCF_3)$ and $[Cp^*Mo(dppe)H_4]^+$ was observed. When using 0.5 equivalents, the resonances corresponding to the tetrahydride complex and trihydride residual starting compound were separate and relatively sharp, see Figure 7a, a similar situation to that seen in CD_2Cl_2 using TFA as proton donor or in THF-d_8 using HBF_4. This indicates that the degenerate exchange is slow under these conditions contrary to the situations in THF-d_8 and C_6D_6 using TFA as proton donor. In turn, this suggests that weak ion pairing occurs, if any, between the tetrahydrido cation and the trifluoroacetate anion in MeCN-d_3. The conversion of the tetrahydride complex to $Cp^*Mo(dppe)H_2(O_2CCF_3)$ is relatively fast and quantitative, see Figure 7b-d. As already noted, when the reaction is carried out in THF the final product is the trifluoroacetate compound rather than the solvent adduct $[Cp^*Mo(dppe)H_2(MeCN)]^+$ (previously shown to result from the interaction with HBF_4), implying that the ligand exchange shown in Equation 2 is completely displaced toward the right.

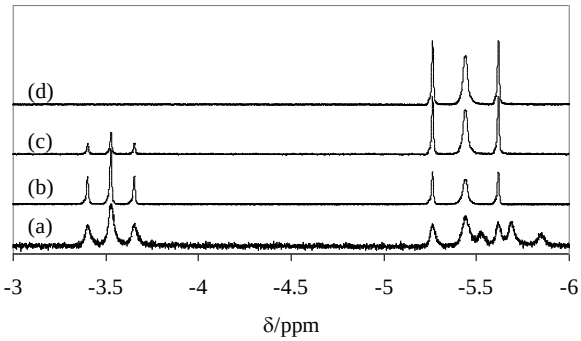

Figure 7. ^{1}H NMR study of the Cp*Mo(dppe)H_3-TFA reaction in MeCN-d_3 at room temperature: (a) 0.5 equiv of TFA, recorded immediately; (b) 1 equiv of TFA, recorded immediately; (c) after 9 min from spectrum (b); (d) 40 min after spectrum (b).

$$Cp^*Mo(dppe)H_2(S)^+ + CF_3COO^- \longrightarrow Cp^*Mo(dppe)H_2(O_2CCF_3) + S$$

(S = THF, MeCN)

Equation 2

A first comparison of the behavior of $[Cp^*Mo(dppe)H_4]^+$ in non coordinating solvents confirms the complex instability, as previously shown for the BF_4^- salt, leading to hydride-free decomposition products.[14] However, in the presence of either coordinating solvents or the CF_3COO^- anion, efficient trapping of the 16-electron product of H_2 dissociation, $[Cp^*Mo(dppe)H_2]^+$, is achieved. The coordinating CF_3COO^- anion is an even better trap than THF and MeCN. The nature of the solvent has a dramatic effect on two related features: (*i*) the ability of the CF_3COO^- anion to attack the cationic complex and yield the neutral dihydride-trifluroacetate product; (*ii*) the rate of degenerate exchange between Cp*Mo(dppe)H_3 and $[Cp^*Mo(dppe)H_4]^+$. The way in which these two processes are affected by the solvent properties will be addressed in more detail in a later section.

(d) IR studies.

As equilibrium positions and reaction rates are expected to strongly depend on the solvent ability to influence hydrogen bonding and ion pairing equilibria, we considered that additional useful information could be gathered from infrared investigations, especially at low temperature where ion pairing and hydrogen bonding are favored. The dielectric permittivity, ε, increases at ambient temperature in the order toluene (2.4) < THF (7.8) < CH_2Cl_2 (8.3) << MeCN (35.9).[24] It increases substantially upon cooling for some solvents, e.g. a values of 15.5 for CH_2Cl_2[25, 26] and 11.9 for THF[27, 28] are recorded at 200 K, but not for others, *e.g.* 2.47 at 240 K and 2.71 at 180 K for toluene.[26] On the other hand, these solvents have different coordinating and acid/base properties. THF is quite an efficient hydrogen bond acceptor (E_j = 1.04), better than MeCN (E_j = 0.75),[29] although the latter is generally a better ligand for transition metals. Benzene and toluene are much weaker bases (E_j = 0.4),[29] whereas CH_2Cl_2 tends to behave more like a weak proton donor than a proton acceptor.[24] We start by presenting the spectral features of the TFA proton donor in the ν_{CO} region in various solvents, since the TFA/solvent interaction certainly plays an important role in the proton transfer equilibria involving the hydride complex. The relevant spectra are shown in Figure 8. Two bands at similar frequencies are observed in CH_2Cl_2 and toluene (1804 and 1785 cm^{-1} for the former, 1803 cm^{-1} and 1788 cm^{-1} for the latter). The higher frequency band is due to the acid monomer, whereas the lower frequency one is typically assigned to the corresponding dimer.[30] Note that the equilibrium is shifted towards the dimer in toluene, as is evident from the different relative intensities. In THF the wide, asymmetric ν_{CO} band of the acid monomer is greatly red-shifted to 1780 cm^{-1} due to the formation of stronger hydrogen bonds to solvent molecules. The shoulder at 1762 cm^{-1} (which becomes a distinct band at 200 K), is assigned to the CF_3COOH dimer. The low-frequency asymmetry of the acid bands in all solvents suggests the presence of higher order TFA associates. Thus THF can form hydrogen bonds with the CF_3COOH, lowering the activity of the acid, which is one of the reasons for the evolution of $Cp^*Mo(dppe)H_4^+CF_3COO^-$ to the final dihydride product in this solvent, as will be shown below.

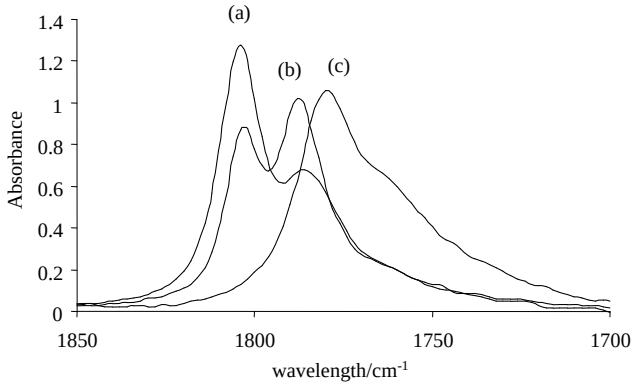

Figure 8. IR spectra of trifluoroacetic acid solutions (0.027 M, pathlength 0.04 mm) in various solvents at 290 K: (a) CH_2Cl_2; (b) toluene; (c) THF.

d1. In dichloromethane. Although the starting material and products are unstable in dichloromethane at room temperature, they do not decompose at low temperatures and this solvent has many advantages for infrared studies (it is not a strong proton acceptor, therefore does not compete with the basic hydride complexes for hydrogen bonding, and has good solvent properties for ionic compounds). An IR monitoring at 200 K in the acid ν_{CO} and conjugated anion ν^{as}_{OCO} vibration region yielded the results shown in Figure 9. At this temperature the dihydride complex Cp*Mo(dppe)H_2(O_2CCF_3), which has a ν^{as}_{OCO} at 1692 cm^{-1} (*vide infra*), does not form.

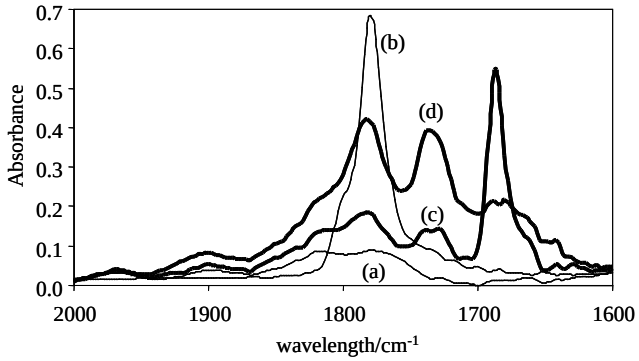

Figure 9. Low temperature (200 K) IR spectra for the reaction between Cp*Mo(dppe)H_3 and TFA in CH_2Cl_2. (a) Cp*Mo(dppe)H_3 (C = 0.028 M); (b) TFA (C = 0.014 M); (c)

mixture of Cp*Mo(dppe)H_3 (C = 0.028 M) and TFA (C = 0.014 M); (d) mixture of Cp*Mo(dppe)H_3 (C = 0.028 M) and TFA (C = 0.028 M).

A tentative assignment of all observed bands is possible on the basis of previous IR studies into the interaction between CF_3COOH and various bases,[30-32] in combination with the results shown in the previous section. At 200K the acid self-association equilibrium is shifted to the dimer, exhibiting a strong band at 1780 cm^{-1} with a shoulder at 1800 cm^{-1}, see Figure 9a. The spectrum recorded for the solution with a MoH_3/TFA ratio of 1:0.5, Figure 9c, shows a prominent band at 1686 cm^{-1}, due to the ν^{as}_{OCO} vibration of the trifluoroacetate anion. Its relatively sharp nature and almost negligible high frequency shift relative to the position of the free CF_3COO^- anion[31, 32] indicates the formation of either a weakly H-bonded contact ion pair or a solvent separated ion pair, consistent with the relatively high polarity of CH_2Cl_2 at low temperatures and the poor proton donor ability of the $[Cp^*Mo(dppe)H_4]^+$ cation. In reference to Scheme 1, this means that species **V** is extensively dissociated to **VI** or that the interaction is loose under these conditions of solvent and temperature. There is no significant intensity in the region characteristic for the free homoconjugate anion, $[CF_3COO(CF_3COOH)_n]^-$. According to the literature, this species should display a low intensity broad band with a maximum at 1630-1620 cm^{-1}.[33] Given the presence of an excess of the trihydride complex, most of the acid is presumably consumed and little is left to yield the homoconjugate anion. The relative intensity of the 1686 cm^{-1} band indicates that the proton transfer equilibrium is highly shifted to the tetrahydride product, and the presence of the unreacted trihydride complex is indicated by the shoulder at 1816 cm^{-1} (*cf.* the starting spectrum of free Cp*Mo(dppe)H_3 in Figure 9b). There are two additional weak bands in this spectrum. The first one at 1782 cm^{-1} could be assigned to free CH_3COOH, but is also consistent with an H-bonded adduct where the acid acts as a proton donor (a CF_3COO-H···B interaction does not significantly perturb the CO normal mode). The second band at 1736 cm^{-1} indicates the presence of an H-bonded adduct where the acid acts as a proton

acceptor (the $CF_3C(OH)O\cdots HA$ interaction significantly red-shifts the CO normal mode).[34, 35] Thus, these bands constitute evidence for the presence of a 2:1 H-bonded adduct, $Cp^*Mo(dppe)H_3\cdots HOOCCF_3\cdots HOOCCF_3$. The simultaneous presence of a 1:1 adduct, $Cp^*Mo(dppe)H_3\cdots HOOCCF_3$, cannot be established because it would also afford a band at ca. 1780 cm^{-1}. A general picture of the proton transfer process can be drawn as shown in Scheme 4.

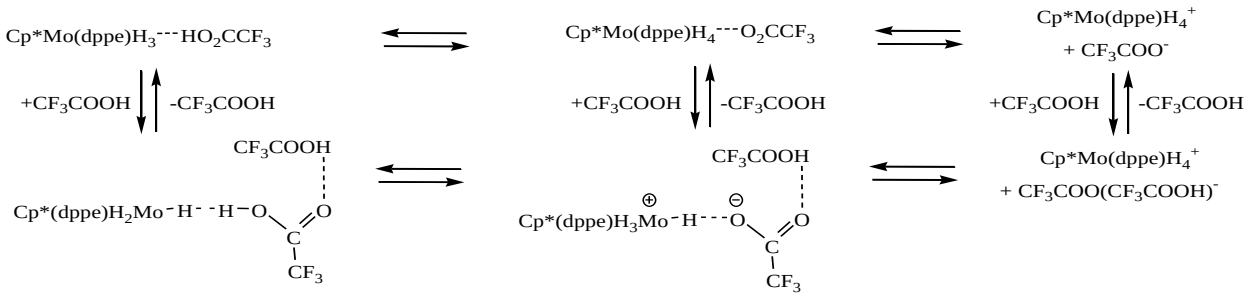

Scheme 4

An increase in the CF_3COOH/MoH_3 ratio is expected to shift the hydrogen bonding equilibrium position towards the 2:1 adduct. At the same time, equilibria involving the anionic species (either hydrogen bonded or free) are expected to shift towards the homoconjugate anion (equilibria drawn vertically in Scheme 4). On the other hand, an increase in the CF_3COOH/MoH_3 ratio will not affect the equilibria shown horizontally in Scheme 4. Indeed, upon addition of a second 0.5 equiv of TFA (final MoH_3/TFA ratio of 1:1), Figure 9d, the IR spectrum reveals a significant increase in intensity for the bands assigned to the neutral 2:1 adduct and a dramatic decrease for that assigned to the free anion. The growth of a broad shoulder at lower frequencies signals the formation of anionic aggregates, as expected.

d2. In benzene/toluene-d_8. The low temperature IR spectral picture in toluene-d_8 in the presence of a stoichiometric amount of TFA is similar to that shown above in dichloromethane, see Figure 10. The band at 1742 cm^{-1} observed for the 1:1 mixture (Figure 10c) is assigned to the ν_{CO} of the hydrogen bonded complex (*cf.* 1736 cm^{-1} in CH_2Cl_2), whereas the bands at 1690

and 1674 cm^{-1} are assigned to the CF_3COO^- anion ($\nu^{as}_{OCO,}$ *cf.* 1686 cm^{-1} in CH_2Cl_2). The complex pattern attained for this absorption is possibly related to the presence of different hydrogen bonded species (H-bonding should be favored more in low polarity toluene). The anion band did not show a significant increase in intensity at greater MoH_3/TFA ratios (1:0.5 or 1:0.2), indicating that the proton transfer equilibrium is shifted further toward the neutral hydrogen bonded species in this solvent in comparison to CH_2Cl_2. This agrees with the results of the NMR investigation. Upon warming above 270 K, the bands corresponding to the $Cp^*Mo(dppe)H_2(O_2CCF_3)$ product at 1702 and 1690 cm^{-1} quickly grow, while the shoulder at 1674 cm^{-1} disappears. The final spectrum is shown in Figure 10d. Monitoring the growth of this band for the 1:1 reaction in C_6H_6 at 298 K (Figure S3 in the Supporting Information) yielded a first order rate constant of $(1.8 \pm 0.1)\cdot10^{-3}$ s^{-1}. In the presence of a 3-5fold excess of acid, the broad, low intensity ν^{as}_{OCO} band of the homoconjugated anion was observed at ca 1640 cm^{-1}. No formation of $Cp^*MoH_2(CF_3COO)(dppe)$ was observed under these conditions, in agreement with the NMR data.

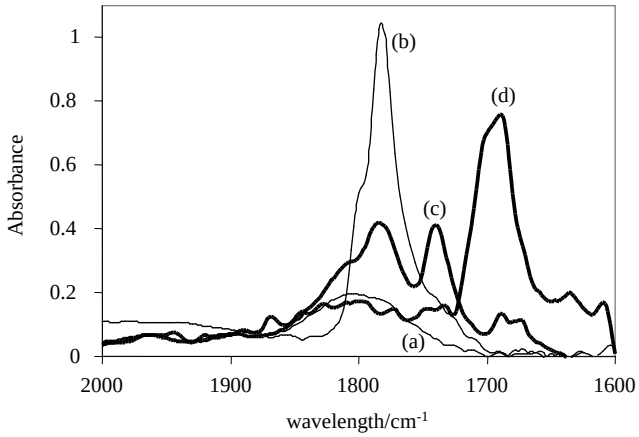

Figure 10. IR spectra for the reaction between $Cp^*Mo(dppe)H_3$ and TFA in toluene-d_8. (a) $Cp^*Mo(dppe)H_3$ (0.027 M) at 200 K; (b) TFA (C = 0.027 M) at 200 K; (c) 1:1 mixture (0.027 M) at 200 K; (d) same mixture as (c), after complete conversion at room temperature.

d3. In THF. At low temperature in this solvent and in the presence of 1 equiv of TFA, the dominant species are the neutral hydrogen bonded complexes, as indicated by the major bands at 1784 and 1744 cm^{-1}, see Figure 11c. No significant amounts of the CF_3COO^- ion can be seen. This implies that proton transfer occurs to a smaller degree than in toluene. No homoconjugated anion band was observed upon raising the TFA excess to 5 equiv, in contrast to the results in aromatic hydrocarbon solution. Upon warming, the spectral changes were similar to those observed in toluene (see previous section), yielding $Cp^*Mo(dppe)H_2(O_2CCF_3)$, Figure 11d. We have also investigated the reverse proton transfer reaction by mixing together $[Cp^*Mo(dppe)H_4]^+BF_4^-$ (generated *in situ* at 200 K from $Cp^*Mo(dppe)H_3$ and HBF_4) and CF_3COONa at 200 K in THF. This experiment confirms the reversible nature of the proton transfer process and the position of equilibrium. The essentially complete disappearance of the trifluoroacetate anion ν^{as}_{OCO} bands at 1702 and 1690 cm^{-1} and the growth of the ν_{CO} band at 1752 cm^{-1} corresponding to the H-bonded adduct[36] were observed at 200K in the presence of either 1 or 2 equiv of $[Cp^*Mo(dppe)H_4]^+BF_4^-$. Subsequent warming to 290 K led once again to $Cp^*Mo(dppe)H_2(OCOCF_3)$ formation.

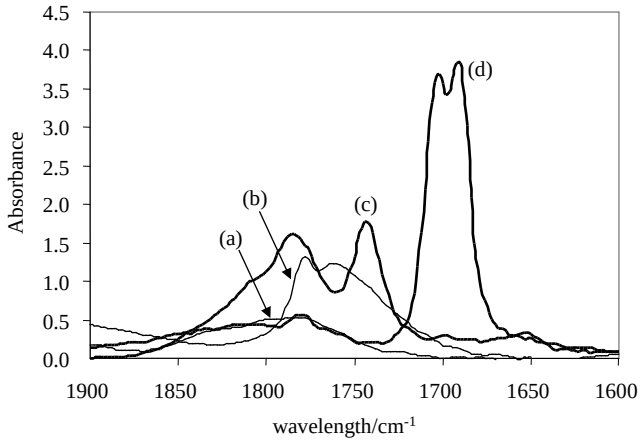

Figure 11. Low temperature (200K) IR spectra for the reaction of $Cp^*Mo(dppe)H_3$ with TFA in THF: (a) Mo complex (C = 0.07 M); (b) TFA (C = 0.07 M); (c) 1:1 mixture (0.07 M) at 200 K; (d) same mixture as (c), after complete conversion at room temperature.

Since the NMR study shows that this conversion also occurs in the presence of excess acid, a kinetics investigation was carried out at 298K using different TFA/Mo ratios. The reaction was found to be zero order with respect to the acid (see Table 3). Interestingly, the rate constant in THF is identical to that measured in benzene (*vide supra*) within experimental error. The study was also extended to different temperatures (using a TFA/Mo ratio of 1:1), the subsequent Eyring analysis (see Supporting Information) giving the following activation parameters: $\Delta H^{\ddagger}$ = 31.8 ± 0.5 kcal mol^{-1} and $\Delta S^{\ddagger}$ = 36 ± 2 e.u. The large positive activation entropy suggests that the transition state is dissociative in nature. At low temperatures, the rearrangement becomes too slow; for instance, reaction rate constants of $5.2 \cdot 10^{-8}$ s^{-1} and $5.8 \cdot 10^{-15}$ s^{-1} are calculated at 250K and 200K, respectively.

Discussion

The collective observations that will be detailed below are summarized in Scheme 5.

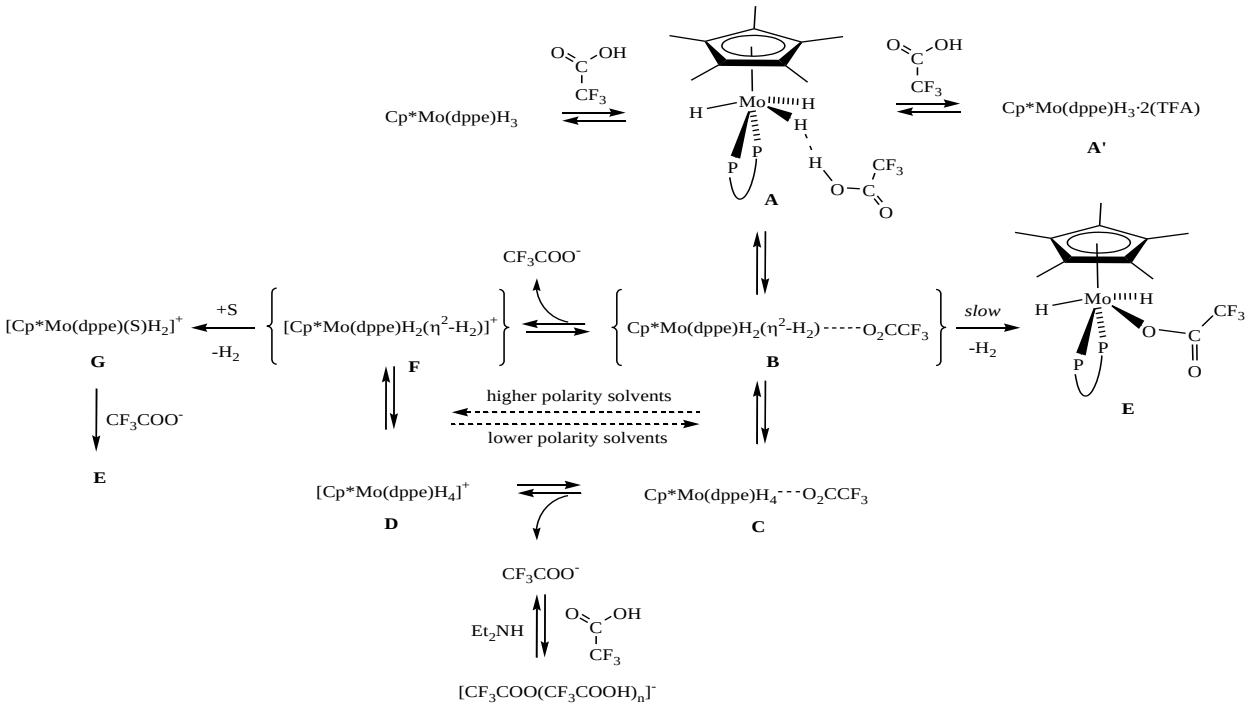

Scheme 5

Proton transfer to $Cp^*Mo(dppe)H_3$, via the H-bonded adduct **A** to yield the classical tetrahydride complex, $[Cp^*Mo(dppe)H_4]^+$, **C/D**, is the only reaction that may occur at low temperatures. The formation of the 2:1 H-bonded adduct **A'** has also been evidenced by low temperature IR, but one molecule of TFA is sufficient for proton transfer to occur, as also indicated by previous kinetics studies.[13] The proton transfer probably proceeds via a nonclassical intermediate (species **B** in Scheme 5), although we have not found any direct experimental evidence to support this proposition. Our recently reported theoretical calculations[13] indicate that the nonclassical complex lies in a very shallow minimum with a low barrier for conversion to the classical tetrahydride product, the isomerization taking place without counteranion dissociation. The competitive dihydrogen evolution yielding $Cp^*Mo(dppe)H_2(O_2CCF_3)$ occurs only above 250 K and is possible (in non coordinating solvents) via the reverse reaction between **D** and CF_3COO^-. This forms the ion pair **C** which subsequently isomerizes to the non-classical species **B**.

The formation of $[Cp^*Mo(dppe)H_4]^+$ is reversible below 250 K in contrast to the irreversible formation of *trans*-$Cp^*MH_2(dppe)^+$ (M = Fe, Ru).[6, 8] One important difference between these systems is the reversibility of the nonclassical/classical isomerization for $[Cp^*Mo(dppe)H_4]^+$ (according to the DFT calculations), whereas this process is irreversible for $[Cp^*M(dppe)H_2]^+$ (M = Fe, Ru). However, proton transfer to the hydride ligand is less thermodynamically favorable for $Cp^*Mo(dppe)H_3$ than for Cp*Fe(dppe)H: a significant amount of TFA remains unreacted (in the H-bonded form) for a TFA/Mo ratio of 0.5 in CH_2Cl_2 at 200K (see Figure 9), whereas it is completely consumed under the same solvent, temperature and stoichiometry conditions in the presence of Cp*Fe(dppe)H.[5] These results contrast with the higher basicity factor of $Cp^*Mo(dppe)H_3$ (E_j = 1.42±0.02)[13] relative to Cp*Fe(dppe)H (E_j = 1.36±0.02).[7] The corresponding proton transfer to Cp*Ru(dppe)H (E_j = 1.39), however, is also an equilibrium process.[6] The basicity factor correlates with the strength of the hydrogen bond

(formation enthalpy), whereas the protonation equilibrium is determined by the free energy of the proton transfer process. Obviously, the two parameters do not necessarily correlate quantitatively.

Both the **A** ↔ **C/D** equilibrium position and rate of the irreversible $Cp^*Mo(dppe)H_2(O_2CCF_3)$ formation depend on the temperature, the solvent and the MoH_3/TFA ratio. Polar solvents (*e.g.* dichloromethane at low temperatures, acetonitrile) weaken the H-bond in **C** and lead to the formation of a solvent separated ion pair (**D** in Scheme 5), which stabilizes the tetrahydrido complex against the H_2 loss. The proton transfer equilibrium is shifted to species **D** in CH_2Cl_2 even in the presence of stoichiometric amounts of the acid. Low polarity solvents (*e.g.* toluene) provide less stabilization for the charged species, thus the proton transfer equilibrium is shifted to the left when near stoichiometric amounts of the acid are used. The tetrahydride product exists as an ion pair stabilized by hydrogen bonding to the CF_3COO^- anion (species **C** in Scheme 5), as reflected for instance in a reduced rate of hydride site exchange measured by ^1H NMR below 240 K. The formation of hydrogen bonded ion pairs of 1:1 composition was also confirmed for weaker proton donors.[13] At room temperature and above, the competitive irreversible H_2 elimination process eventually leads to the quantitative formation of the final product **E**. However, excess acid favors ion pair dissociation through formation of the thermodynamically more stable homoconjugate anion, thereby stabilizing the proton transfer product **D** and precluding the H_2 evolution.

In solvents with proton accepting ability (THF, MeCN) the activity of the acid is reduced by H-bonding with solvent molecules, formation of the homoconjugated anion is not observed and the reaction yields **E** even in the presence of excess acid. The attainment of the same formation rate constant in THF and in benzene and the zero order dependence on TFA agree with the proposed unimolecular generation of **E** from the same intermediate **B**. Furthermore, the large positive activation entropy is consistent with a dissociative mechanism (i.e. H_2 must leave before the trifluoroacetate anion can coordinate), as may be expected from the

electronically saturated nature of system **B**. The rate of formation in MeCN has not been determined with accuracy, but the NMR data in Figure 7 allow us to estimate a rate constant of ca. $2 \cdot 10^{-3}$ s^{-1}, *i.e.* close to that determined in THF and benzene (see Table 3) , if we assume a first order decay process is in operation. The high polarity of MeCN favors proton transfer and ion pair dissociation through the stabilization of the charge-separated species, but the instability of $[Cp^*Mo(dppe)H_4]^+$ leads to its ultimate decomposition by H_2 elimination. In this case, the process may be solvent-assisted, leading to the solvent adduct **G**, as previously established by the protonation with HBF_4.[14] This phenomenon also occurs in THF as verified by using HBF_4. However, the CF_3COO^- anion has a stronger coordinating power than both THF and MeCN and the ultimate product is once again **E**.

Species **A** and **C/D** exhibit a dynamic exchange process, as revealed by a broad ^1H NMR resonance at room temperature which decoalesces at 270 K in $C_6D_5CD_3$ for the mixture containing 1 equiv of TFA. This results from the fast and direct unimolecular proton transfer involving the dihydrogen bonded complex **A** and the H-bonded ion pair **C**. It is not possible, unfortunately, to use this information to derive an accurate value for the proton transfer rate constant, because of the complexity of the coupled equilibria and the irreversible transformation to product **E**. Assuming, however, that only species **A** and **C** are present in an approximately equimolar ratio, an activation barrier $\Delta G^{\ddagger}$ of 11.7 kcal mol^{-1} may be estimated for the proton transfer in $C_6D_5CD_3$ at 270 K, from the coalescence temperature and the chemical shift difference.[37] This activation barrier is lower than that of the proton transfer by HFIP in toluene ($\Delta G^{\ddagger}_{293K}$ = 15.8 kcal mol^{-1}),[13] in agreement with the higher proton donating ability of TFA. It is also lower than $\Delta G^{\ddagger}_{270K}$ for the proton transfer from HFIP to Cp*Fe(dppe)H in CH_2Cl_2 (14.7 kcal mol^{-1}) or from PFTB to CpRuH(CO(PCy_3) in hexane (16.1 kcal mol^{-1}), calculated for 270 K using the published activation parameters.[3, 5] IR kinetic data (*vide supra*) give $\Delta G^{\ddagger}_{270K}$ = 22.1

kcal mol^{-1} for the dihydrido-trifluoroacetate formation. The irreversibility of the H_2 evolution process renders $Cp^*Mo(dppe)H_2(O_2CCF_3)$ the sole end product.

A final point of interest is a comparison between the results shown here and those reported previously for the decomposition of the proton transfer product obtained with TFE, which led to a diamagnetic hydride-free decomposition product, $Cp^*Mo(dppe)(OCH_2CF_3)(TFE)_x$ (x = 0 or 1). The mechanism is likely to be the same for both systems, leading to a first H_2 elimination assisted by the coordination of the alkoxide ligand, see Scheme 6. Why does $Cp^*Mo(dppe)H_2(O_2CCF_3)$ show no tendency to expel a second H_2 molecule and form the hypothetical compound $Cp^*Mo(dppe)(O_2CCF_3)$, in which the trifluoroacetate ligand would bind in a chelating fashion, whereas $[Cp^*Mo(dppe)H_4]^+(^-OCH_2CF_3)$ leads to a hydride-free product without the observation of even trace amounts of a dihydride intermediate? A possible rationalization is that the stronger π-donating ability of the oxygen lone pairs in the fluorinated alkoxide ligand may assist the elimination of the second H_2 molecule by stabilizing the resulting 16-electron half-sandwich Mo^{II} product. By contrast, the lone pair of the trifluoroacetate oxygen donor atom is not sufficiently basic and the second oxygen atom is presumably not capable of assisting the H_2 elimination process, due to either thermodynamic or kinetic reasons.

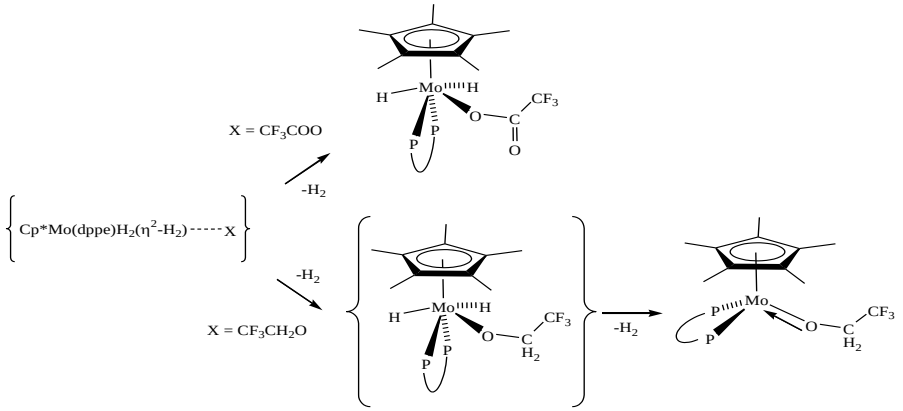

Scheme 6

Conclusion

We have explored the protonation of Cp*Mo(dppe)H_3 by trifluoroacetic acid in various solvents which display different proton accepting ability, polarity, and coordinating power toward transition metals: dichloromethane, benzene/toluene, THF and MeCN. The nature of the solvent and the amount of excess acid determine the nature of the product by delicately controlling the position of the proton transfer and ion pairing equilibria. In agreement with previous investigations, the classical tetrahydrido cation is produced following the initial formation of a dihydrogen bonded intermediate without the observation of a nonclassical tautomer (dihydrogen complex); it is stable at low temperatures, and can exist as solvent separated or contact ion pair. However, the use of suitable conditions of solvent, temperature and hydride/acid ratio has led to the selective formation of a new product, the dihydrido complex Cp*Mo(dppe)$H_2(O_2CCF_3)$. The trifluoroacetate anion is a sufficiently strong ligand to coordinate the cationic complex and saturate its coordination sphere after loss of H_2, even in the presence of coordinating solvent molecule such as MeCN or THF. However, it remains coordinated in a monodentate fashion and, contrary to the $CF_3CH_2O^-$ anion, is not capable of inducing the elimination of the residual hydride ligands as H_2 to form a hydride-free product.

Experimental section

General. All manipulations were performed under an argon atmosphere by standard Schlenk techniques. All solvents were dried over appropriate drying agent (Na/benzophenone for benzene, toluene or THF, Na for pentane, CaH_2 for CH_2Cl_2) and freshly distilled under an argon atmosphere prior to use. C_6D_6, $C_6D_5CD_3$, THF-d_8, CD_3CN, CD_2Cl_2 by Euriso-Top for NMR experiments and $C_6D_5CD_3$ by Aldrich for IR experiments were degassed by three freeze-pump-thaw cycles, and then purified by vacuum transfer at room temperature. Cp*Mo(dppe)H_3 was synthesized according to literature.[14]

Spectroscopic studies. (a) NMR investigations. Samples of the hydride Cp*Mo(dppe)H_3 in each solvent were prepared under an argon atmosphere in 5 mm NMR tubes. The ^{1}H and ^{31}P{^{1}H} data were collected with Bruker AMX300 and Bruker AV500 spectrometers, operating at 300.1 (500.3) MHz and 121.5 (202.5) MHz, respectively. The temperature was calibrated using a methanol chemical shift thermometer; the accuracy and stability was ±1 K. All samples were allowed to equilibrate at every temperature for at least 3 min. The spectra were calibrated with the residual solvent resonance (^{1}H) and with external 85% H_3PO_4 (^{31}P). The conventional inversion-recovery method (180-τ-90) was used to determine the variable-temperature longitudinal relaxation time T_1. Standard Bruker software was used for the calculation of the longitudinal relaxation time.

(b) IR Investigations. The IR measurements were performed on the "Infralum 801" FT-IR spectrometer using CaF_2 cells of 0.04 cm path length. All IR measurements were carried out by use of a home-modified cryostat (Carl Zeiss Jena) in the 190-290 K temperature range. The cryostat modification allows operating under an inert atmosphere and transferring the reagents (premixed either at low or room temperature) directly into the cell pre-cooled to the required temperature. The accuracy of the temperature adjustment was ±1 K. This setup was used both for the variable-temperature studies and for the kinetics investigations.

Synthesis of Cp*Mo(dppe)H_2(O_2CCF_3). A CF_3COOH solution (9.5 μL, 0.13 mmol) in THF (3 mL) was slowly added to a solution of Cp*Mo(dppe)H_3 (80 mg, 0.13 mmol) in 15 mL THF. The reaction mixture was stirred at RT for ca. 1.5 h. The solvent was evaporated and the resulting solid was recrystallized from pentane. Yield: 75 mg (78%). ^{1}H NMR (300.13 MHz, C_6D_6, 290K): δ -5.09 (Mo-H_2), 1.79 (s, 15 H, Cp*), 3.2-2.5 (m, 4 H, -CH_2-CH_2-), 7.10-7.77 (m, 20 H, Ph). ^{31}P {^{1}H} NMR (121.5 MHz, C_6D_6, 290K): δ 76.9 (s). The ^{1}H hydride and the ^{31}P resonances decoalesce at low temperatures (see Results and discussion section). IR (KBr), cm^{-1}: 1682 and 1702 (sh) (ν_{CO}), 1818 and 1850 (Mo-H_2). *Anal*. Calc. for $C_{38}H_{41}F_3P_2O_2Mo$: C, 61.29;

H, 5.56. Found: C, 61.26; H, 5.54. Crystals were grown by slow diffusion of a pentane layer into a saturated solution of the mixture Cp*Mo(dppe)H_3 and ca. 1 equiv TFA in toluene.

Kinetics of the Cp*Mo(dppe)$H_2(O_2CCF_3)$ formation. The reagents were mixed at low temperature (ca. 270 K) and the solution was transferred into the cryostat. The kinetics data were obtained by following the increase of the band at 1692 cm^{-1} corresponding to the Cp*Mo(dppe)$H_2(O_2CF_3)$ complex at the desired temperature. The first-order rates were obtained by plotting $\ln(A_\infty - A_t)$ vs. time.

X-ray analysis of compound Cp*Mo(dppe)$H_2(O_2CCF_3)$. Single crystal was mounted under inert perfluoropolyether on the tip of glass fibre and cooled in the cryostream of the Oxford-Diffraction XCALIBUR CCD diffractometer. Data were collected using the monochromatic MoKα radiation (λ= 0.71073). The structure was solved by direct methods (SIR97)[38] and refined by least-squares procedures on F^2 using SHELXL-97.[39] All H atoms attached to carbon were introduced in calculation in idealised positions and treated as riding models. The two hydrides were located in difference Fourier syntheses and they were freely refined with isotropic thermal parameter. The drawing of the molecule was realised with the help of ORTEP32.[40] Crystal data and refinement parameters are shown in Table 2. Crystallographic data (excluding structure factors) have been deposited with the Cambridge Crystallographic Data Centre as supplementary publication no. CCDC 632317. Copies of the data can be obtained free of charge on application to the Director, CCDC, 12 Union Road, Cambridge CB2 1EZ, UK (fax: (+44) 1223-336-033; e-mail: deposit@ccdc.cam.ac.uk).

Acknowledgment

We thank the European Commission through the HYDROCHEM program (contract HPRN-CT-2002-00176) for support of this work. Additional bilateral support (PICS, France-Russia) and National support from the CNRS (France), from the RFBR (05-03-22001, 05-03-32415) and the Division of Chemistry and Material Sciences of RAS (Russia), is also gratefully

acknowledged. NB thanks Russian Science Support Foundation for an individual grant. MB thanks the Spanish Ministerio de Educación y Ciencia for a post-doctoral fellowship.

Supporting Information

Table of longitudinal relaxation times at different temperatures for the hydride resonance of $Cp^*Mo(dppe)H_2(O_2CCF_3)$ and figures showing IR spectra of this compound in various solvents, the IR study of its formation kinetics in toluene, and an Eyring plot of the rate constants in THF (4 pages).

References

[1] N. V. Belkova, E. S. Shubina, L. M. Epstein, *Acc. Chem. Res.* **2005**, *38*, 624.

[2] N. V. Belkova, A. V. Ionidis, L. M. Epstein, E. S. Shubina, S. Gruendemann, N. S. Golubev, H. H. Limbach, *Eur. J. Inorg. Chem.* **2001**, 1753.

[3] N. Belkova, M. Besora, L. Epstein, A. Lledós, F. Maseras, E. Shubina, *J. Am. Chem. Soc.* **2003**, *125*, 7715.

[4] E. Gutsul, N. Belkova, G. Babakhina, L. Epstein, E. Shubina, C. Bianchini, M. Peruzzini, F. Zanobini, *Russ. Chem. Bull.* **2003**, *52*, 1204.

[5] N. V. Belkova, E. Collange, P. Dub, L. M. Epstein, D. A. Lemenovskii, A. Lledós, O. Maresca, F. Maseras, R. Poli, P. O. Revin, E. S. Shubina, E. V. Vorontsov, *Chem. Eur. J.* **2005**, *11*, 873.

[6] N. V. Belkova, P. A. Dub, M. Baya, J. Houghton, *Inorg. Chim. Acta* **2007**, *360*, 149–162.

[7] N. V. Belkova, P. O. Revin, L. M. Epstein, E. V. Vorontsov, V. I. Bakhmutov, E. S. Shubina, E. Collange, R. Poli, *J. Am. Chem Soc.* **2003**, *125*, 11106.

[8] M. Baya, O. Maresca, R. Poli, Y. Coppel, F. Maseras, A. Lledós, N. V. Belkova, P. A. Dub, L. M. Epstein, E. S. Shubina, *Inorg. Chem.* **2006**, *45*, 10248.

[9] M. S. Chinn, D. M. Heinekey, *J. Am. Chem. Soc.* **1990**, *112*, 5166.

[10] E. S. Shubina, N. V. Belkova, E. V. Bakhmutova, E. V. Vorontsov, V. I. Bakhmutov, A. V. Ionidis, C. Bianchini, L. Marvelli, M. Peruzzini, L. M. Epstein, *Inorg. Chim. Acta* **1998**, *280*, 302.

[11] N. V. Belkova, E. S. Shubina, E. I. Gutsul, L. M. Epstein, I. L. Eremenko, S. E. Nefedov, *J. Organomet. Chem.* **2000**, *610*, 58.

[12] S. Gründeman, S. Ulrich, H.-H. Limbach, N. S. Golubev, G. S. Denisov, L. M. Epstein, S. Sabo-Etienne, B. Chaudret, *Inorg. Chem.* **1999**, *38*, 2550.

[13] N. V. Belkova, P. O. Revin, M. Besora, M. Baya, L. M. Epstein, A. Lledós, R. Poli, E. S. Shubina, E. V. Vorontsov, *Eur. J. Inorg. Chem.* **2006**, 2192.

[14] B. Pleune, R. Poli, J. C. Fettinger, *Organometallics* **1997**, *16*, 1581.

[15] J. Andrieu, N. V. Belkova, M. Besora, E. Collange, L. M. Epstein, A. Lledós, R. Poli, P. O. Revin, E. S. Shubina, E. V. Vorontsov, *Russ. Chem. Bull.* **2003**, *52*, 2679.

[16] J. H. Shin, D. G. Churchill, G. Parkin, *J. Organomet. Chem.* **2002**, *642*, 9.

[17] E. Le Grognec, R. Poli, P. Richard, *Organometallics* **2000**, *19*, 3842.

[18] M. A. A. F. D. C. T. Carrondo, M. J. Calhorda, M. B. Hursthouse, *Acta Crystallogr., Sect. C: Cryst. Struct. Commun.* **1987**, *C43*, 880.

[19] T. Steiner, *Journal of Chemical Crystallography* **1999**, *29*, 1235.

[20] L. M. Epstein, L. N. Saitkulova, G. P. Zol'nikova, D. N. Kravtsov, *Metalloorganicheskaya Khimiya* **1991**, *4*, 1368.

[21] Footnote3.

[22] Footnote2.

[23] E. S. Shubina, N. V. Belkova, A. N. Krylov, E. V. Vorontsov, L. M. Epstein, D. G. Gusev, M. Niedermann, H. Berke, *J. Am. Chem. Soc.* **1996**, *118*, 1105.

[24] C. Reichardt, *Solvents and Solvent Effects in Organic Chemistry*, 3rd ed., WILEY-VCH, Weinheim, **2003**.

[25] S. O. Morgan, H. H. Lowry, *J. Phys. Chem.* **1930**, *34*, 2385.

[26] S. Sharif, G. S. Denisov, M. D. Toney, H.-H. Limbach, *J. Am. Chem. Soc.* **2006**, *128*, 3375.

[27] C. Carvajal, K. J. Tolle, J. Smid, M. Szwarc, *J. Am. Chem. Soc.* **1965**, *87*, 5548.

[28] D. J. Metz, A. Glines, *J. Phys. Chem.* **1967**, *71*, 1158.

[29] A. V. Iogansen, *Theor. Experim. Khim.*, **1971**, *7*, 302.

[30] J. Z. Dega-Szafran, M. Grundwald-Wyspianska, M. Szafran, *Spectrochim. Acta* **1991**, *47A*, 543.

[31] L. M. Epstein, A. N. Krylov, E. S. Shubina, *J. Mol. Struct.* **1994**, *322*, 345.

[32] E. S. Shubina, A. N. Krylov, N. V. Belkova, L. M. Epstein, A. P. Borisov, V. D. Mahaev, *J. Organometal. Chem.* **1995**, *493*, 275.
[33] W. Klemperer, G. C. Pimentel, *J. Chem. Phys.* **1954**, *22*, 1399.
[34] J. P. Castaneda, G. S. Denisov, S. Y. Kucherov, V. M. Schreiber, A. V. Shurukhina, *J. Mol. Struct.* **2003**, *660*, 25–40.
[35] G. V. Gusakova, G. S. Denisov, A. L. Smolyanskii, *Optika i Spektroskopiya* **1972**, *32*, 922.
[36] Footnote1.
[37] J. Sandström, *Dynamic NMR Spectroscopy*, Academic Press, London, **1982**.
[38] A. Altomare, M. Burla, M. Camalli, G. Cascarano, C. Giacovazzo, A. Guagliardi, A. Moliterni, G. Polidori, R. Spagna, *J. Appl. Cryst.* **1999**, *32*, 115.
[39] G. M. Sheldrick, *SHELXL97. Program for Crystal Structure refinement*, University of Göttingen, Göttingen, Germany, **1997**.
[40] L. J. Farrugia, *J. Appl. Crystallogr.* **1997**, *32*, 565.

Table 1. Selected bond distances (Å) and angles (°) for compound $Cp^*Mo(dppe)H_2(OCOCF_3)$.

Mo(1)-CNT	1.96462(17)	Mo(1)-O(1)	2.2008(15)
Mo(1)-P(1)	2.5206(5)	Mo(1)-P(2)	2.3962(5)
Mo(1)-H(1)	1.60(3)	Mo(1)-H(2)	1.65(3)
P(1)-C(111)	1.833(2)	P(2)-C(211)	1.8459(19)
P(1)-C(121)	1.834(2)	P(2)-C(221)	1.828(2)
P(1)-C(6)	1.844(2)	P(2)-C(7)	1.849(2)
C(6)-C(7)	1.526(3)	C(8)-C(9)	1.547(3)
C(8)-O(1)	1.249(3)	C(8)-O(2)	1.221(3)

CNT-Mo(1)-O(1)	119.74(4)		
P(2)-Mo(1)-P(1)	81.360(17)	H(2)-Mo(1)-H(1)	105.6(14)
CNT-Mo(1)-P(1)	122.648(13)	CNT-Mo(1)-P(2)	144.369(14)
O(1)-Mo(1)-P(1)	76.82(4)	O(1)-Mo(1)-P(2)	89.40(4)
CNT-Mo(1)-H(1)	98.5(10)	CNT-Mo(1)-H(2)	96.9(9)
O(1)-Mo(1)-H(1)	139.8(10)	O(1)-Mo(1)-H(2)	83.0(10)
P(2)-Mo(1)-H(1)	61.6(10)	P(2)-Mo(1)-H(2)	64.6(9)
P(1)-Mo(1)-H(1)	72.0(11)	P(1)-Mo(1)-H(2)	140.5(9)

Table 2. Characteristics of the ν^{as}_{OCO} band of Cp*Mo(dppe)H_2($OCOCF_3$) in the solid state and in solution.

solvent	ν^{as}_{OCO} /cm^{-1}	$\Delta\nu$	intensity ratio (A_{low}/A_{high})
solid (KBr)	1700 sh, 1685 s	15	1.8
C_6H_6	1700 sh, 1690	10	1.2
$C_6D_5CD_3$	1700 sh, 1690	10	1.1
THF	1702, 1690	12	1.0
CH_2Cl_2	1706 sh, 1688	18	2.2

Table 3. Rate constants for the Cp*Mo(dppe)H_2(O_2CCF_3) formation reaction in THF. C(MoH_3) = 0.025 M.

T, K	TFA/Mo	k, 10^{-3} s^{-1}
280	1	0.064 ± 0.0015
290	1	0.63± 0.01
298	0.5	1.7 ± 0.1
298	1	1.8 ± 0.1
298	3	1.9 ± 0.1
298	5	1.80 ± 0.05
308	1	13.7 ± 0.2

Table 4. Crystal data and structure refinement for compound $Cp^*Mo(dppe)H_2(O_2CCF_3)$

Empirical formula	$C_{38}H_{41}F_3MoO_2P_2$	
Formula weight	744.59	
Temperature	180(2) K	
Wavelength	0.71073 Å	
Crystal system	Monoclinic	
Space group	$P\ 2_1/n$	
Unit cell dimensions	a = 11.2103(4) Å	α= 90°.
	b = 15.0429(7) Å	β= 93.675(3)°.
	c = 20.1563(7) Å	γ = 90°.
Volume	3392.1(2) $Å^3$	
Z	4	
Density (calculated)	1.458 Mg/m^3	
Absorption coefficient	0.531 mm^{-1}	
F(000)	1536	
Crystal size	0.57 x 0.3 x 0.28 mm^3	
Theta range for data collection	2.96 to 30.03°.	
Index ranges	-15<=h<=15, -12<=k<=21, -28<=l<=28	
Reflections collected	31116	
Independent reflections	9836 [R(int) = 0.0477]	
Completeness to theta = 30.00°	99.1 %	
Absorption correction	Semi-empirical from equivalents	
Max. and min. transmission	0.9726 and 0.7281	
Refinement method	Full-matrix least-squares on F^2	
Data / restraints / parameters	9836 / 0 / 428	
Goodness-of-fit on F^2	1.082	
Final R indices [I>2sigma(I)]	R1 = 0.0403, wR2 = 0.1022	
R indices (all data)	R1 = 0.0480, wR2 = 0.1072	
Largest diff. peak and hole	1.193 and -1.187 e.$Å^{-3}$	

The outcome of proton transfer from CF_3COOH to $Cp^*Mo(dppe)H_3$ is highly solvent dependent: formation of separated $[Cp^*Mo(dppe)H_4]^+$ and trifluoracetate ions of H_2 evolution with formation of the new $Cp^*Mo(dppe)H_2(OOCCF_3)$ complex.

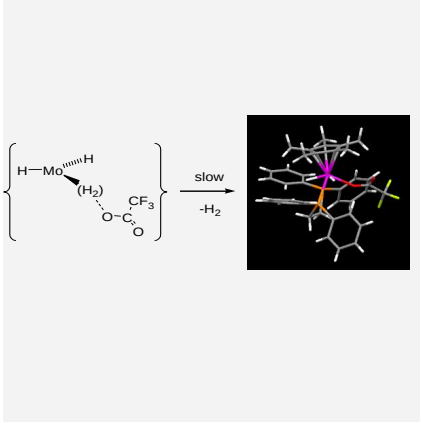

Pavel A. Dub, Miguel Baya, Jennifer Houghton, Natalia V. Belkova, Jean-Claude Daran, Rinaldo Poli,* Lina M. Epstein, Elena S. Shubina* ……..
Page No. XXX – Page No. XXX

Solvent control in the protonation of $Cp^*Mo(dppe)H_3$ by CF_3COOH

Keywords: Molybdenum / hydride ligands / proton transfer / dihydrogen bonding / trifluoroacetate ligand

Hydride protonation

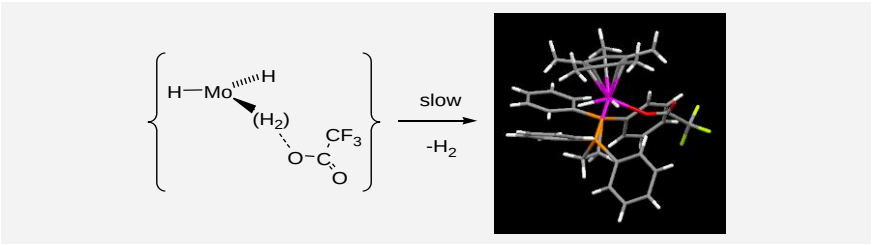

The outcome of proton transfer from CF_3COOH to $Cp^*Mo(dppe)H_3$ is highly solvent dependent: formation of separated $[Cp^*Mo(dppe)H_4]^+$ and trifluoracetate ions of H_2 evolution with formation of the new $Cp^*Mo(dppe)H_2(OOCCF_3)$ complex.

Pavel A. Dub, Miguel Baya, Jennifer Houghton, Natalia V. Belkova, Jean-Claude Daran, Rinaldo Poli,* Lina M. Epstein, Elena S. Shubina* ……..
Page No. XXX – Page No. XXX

Solvent control in the protonation of $Cp^*Mo(dppe)H_3$ by CF_3COOH

Keywords: Molybdenum / hydride ligands / proton transfer / dihydrogen bonding / trifluoroacetate ligand